

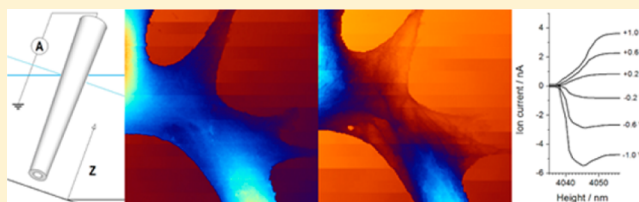
Pipette–Surface Interaction: Current Enhancement and Intrinsic Force

Richard W. Clarke,* Alexander Zhukov, Owen Richards, Nicholas Johnson, Victor Ostanin, and David Klenerman*

Department of Chemistry, University of Cambridge, Lensfield Road, Cambridge, CB2 1EW, United Kingdom

S Supporting Information

ABSTRACT: There is an intrinsic repulsion between glass and cell surfaces that allows noninvasive scanning ion conductance microscopy (SICM) of cells and which must be overcome in order to form the gigaseals used for patch clamping investigations of ion channels. However, the interactions of surfaces in physiological solutions of electrolytes, including the presence of this repulsion, for example, do not obviously agree with the standard Derjaguin–Landau–Verwey–Overbeek (DLVO) colloid theory accurate at much lower salt concentrations. In this paper we investigate the interactions of glass nanopipettes in this high-salt regime with a variety of surfaces and propose a way to resolve DLVO theory with the results. We demonstrate the utility of this understanding to SICM by topographically mapping a live cell's cytoskeleton. We also report an interesting effect whereby the ion current through a nanopipette can increase under certain conditions upon approaching an insulating surface, rather than decreasing as would be expected. We propose that this is due to electroosmotic flow separation, a high-salt electrokinetic effect. Overall these experiments yield key insights into the fundamental interactions that take place between surfaces in strong solutions of electrolytes.



1. INTRODUCTION

Scanning ion conductance microscopy (SICM)¹ uses very fine saline-filled glass pipettes called nanopipettes to map surface topography in solution, allowing 10 nm resolution imaging of live cells.² An ion current through the tip aperture is produced by a voltage applied between the bath solution and the working electrode of a patch-clamp ammeter inserted at the top of the nanopipette, as shown in Figure 1. If an insulating surface largely occludes the aperture when the piezoelectric mounted nanopipette moves downward from bulk solution, then the ion current reduces, allowing the probe to sense the proximity of the surface. We have investigated two related phenomena: How the ion current changes as the nanopipette approaches surfaces and the sign and magnitude of the force it exerts.

Approaches for SICM imaging are usually made up to a set percentage decrease in ion current, typically less than 1%, at which point the tip is approximately one radius of the nanopipette aperture from the surface, between 10 and 25 nm in these experiments. This variation is due to the stochastic manufacturing process: pairs of nanopipettes are made by heating and pulling a glass capillary until it snaps, using a laser-based puller with a carefully tuned program, see Methods section for details. Topographic images are constructed by scanning the sample laterally and registering heights. There are various implementations of SICM control systems,^{3,4} but they all make this assumption that the ion current falls monotonically in magnitude as the probe nears a surface. We show here that in some common circumstances though, most obviously for negative capillary electrode voltages, the size of the ion

current can actually rise before it falls. The effect is unusual electrokinetically because it is still strong at physiological ionic strength. As we discuss in more detail later, this is a consequence of the nanoscale insulating geometry of the tip.

Apart from a decreasing ion current near a surface, SICM also implicitly relies upon another physical assumption in order to map live cells without damaging them, that the glass probe is not monotonically attracted to the cell surface. This is quite crucial because glass adheres to cell membranes very strongly, making possible the GΩ seals required for patch-clamping, for example. Yet if parts of the nanopipette were to adhere like this upon every approach, the cell would be rapidly torn to pieces. Therefore the extensive success of SICM at mapping live cells noninvasively indicates that the pipet must repel the cell membrane. If this repulsion were to occur at a distance of ~0.78 nm, the Debye length in physiological solution, then the usual hypothesis in colloid science would be to suggest that it was due to double-layer repulsion. However, we find here that soft surfaces are pushed away by the glass pipet from distances more than 10 times further away. This greatly assists SICM imaging by preventing cells from being ripped at any millions of approaches, allowing imaging of live cells for hours or days.⁵

We first describe our experimental results on the changes in force and current when nanopipettes approach surfaces in electrolyte. We then discuss possible physical mechanisms that can explain these and other related observations.

Received: September 24, 2012

Published: December 4, 2012



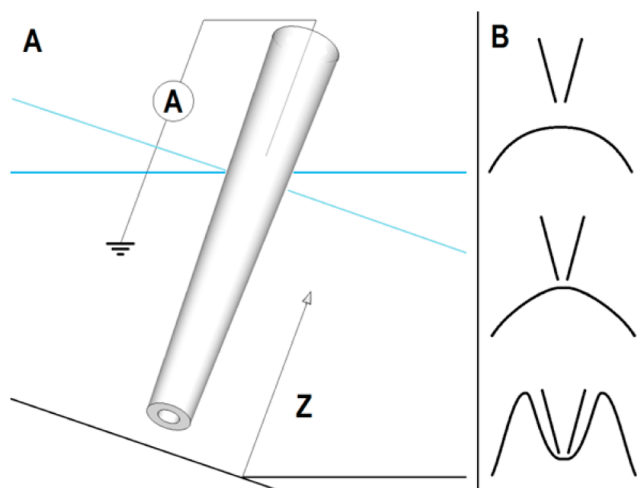


Figure 1. SICM functions by detecting a reduction in ion current when a nanopipette approaches an insulating surface. (A) Nanopipette tips typically have 3° half angle taper and 50 nm radius and aperture diameter. The section in the schematic is 1000 nm long; the rest of the capillary would be 50 000 times longer. The two blue lines represent the solution surface, usually much further away. The patch-clamp amplifier/ammeter applies a voltage, typically 200 mV, between Ag/AgCl electrodes in the bath (ground) and in the capillary. (B) Pipettes push decane droplets without touching them despite a weak initial attraction.

2. METHODS

We set nanopipettes on a vertical 25 μm piezo, and sample surfaces in a 30 μm travel piezo (both Physik Instrumente) stationary for approach experiments but moving in the horizontal plane for imaging. Decane (Sigma-Aldrich) droplets, typically 60 μm in diameter, were dispersed on to the surfaces of Petri dishes (35 mm, untreated polystyrene, Corning) from a diffuser spray bottle (Boots, U.K.) before adding salt solution. Glass slides were cleaned with [7.5% H_2O_2 , 17.5% H_2O , 75% H_2SO_4] piranha solution, and silicone glued under 10 mm diameter holes cut into Petri dishes. Pairs of nanopipettes were pulled from 10 cm fire-polished borosilicate filamented capillaries, 0.50/1.00 mm inner/outer diameter (Sutter, Intracel) using a P-2000 puller (Sutter Instruments), using the following program: [Heat = 350, Fil = 3, Vel = 30, Del = 220, Pul = __; Heat = 390, Fil = 3, Vel = 40, Del = 180, Pul = 255], pull time 4.5–5.5 s. The tips of these nanopipettes typically have a 30 nm inner aperture diameter and a half-cone angle of 3° , giving 300 $\text{M}\Omega$ resistances in 150 mM NaCl. To allow closer experimental approaches to hard surfaces, we flattened tip faces parallel by moving the pipet down at $10\text{ nm}\cdot\text{ms}^{-1}$, hopping up when the ion current first exceeded the value in bulk. This typically increases the ion current by 50%, indicating⁶ an increase in aperture diameter to $\sim 50\text{ nm}$. Tips that broke further up were discarded. Solutions were filtered by Anotop 0.02 μm filters (Whatman). No pressure was applied, and capillary action balanced the weight of the solution column in the pipet. Graphs typical of hundreds of experiments are presented.

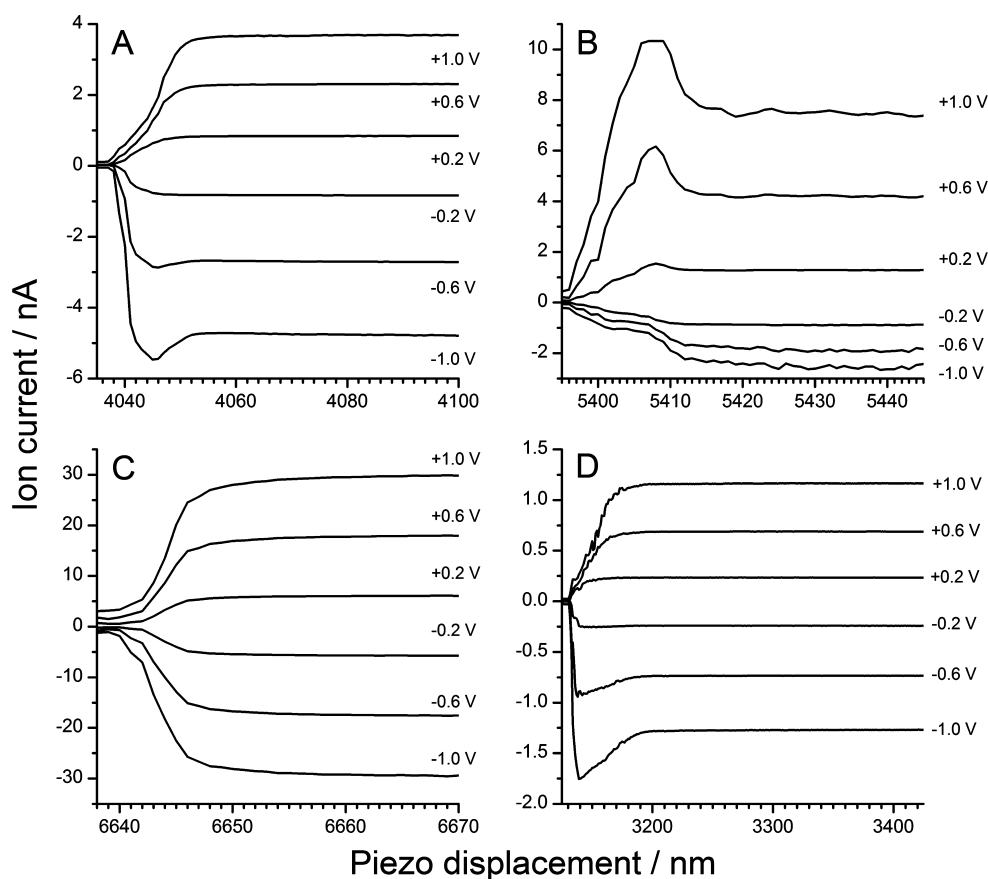


Figure 2. Nanopipette ion current versus height above polystyrene. (A) 150 mM NaCl. The ion current decays monotonically for positive pipet electrode voltages as would be expected for progressive occlusion of the tip aperture by the surface. For negative biases though, the ion current increases first. (B) 150 mM NaCl, 10 ppm w/v polylysine. This reverses the surface charge of the glass, and the polarity of the ion current increases. (C) 1500 mM NaCl. No ion current increases are seen. (D) 15 mM NaCl. The height scale of the negative ion current increase is larger, reflecting the increase in Debye length.

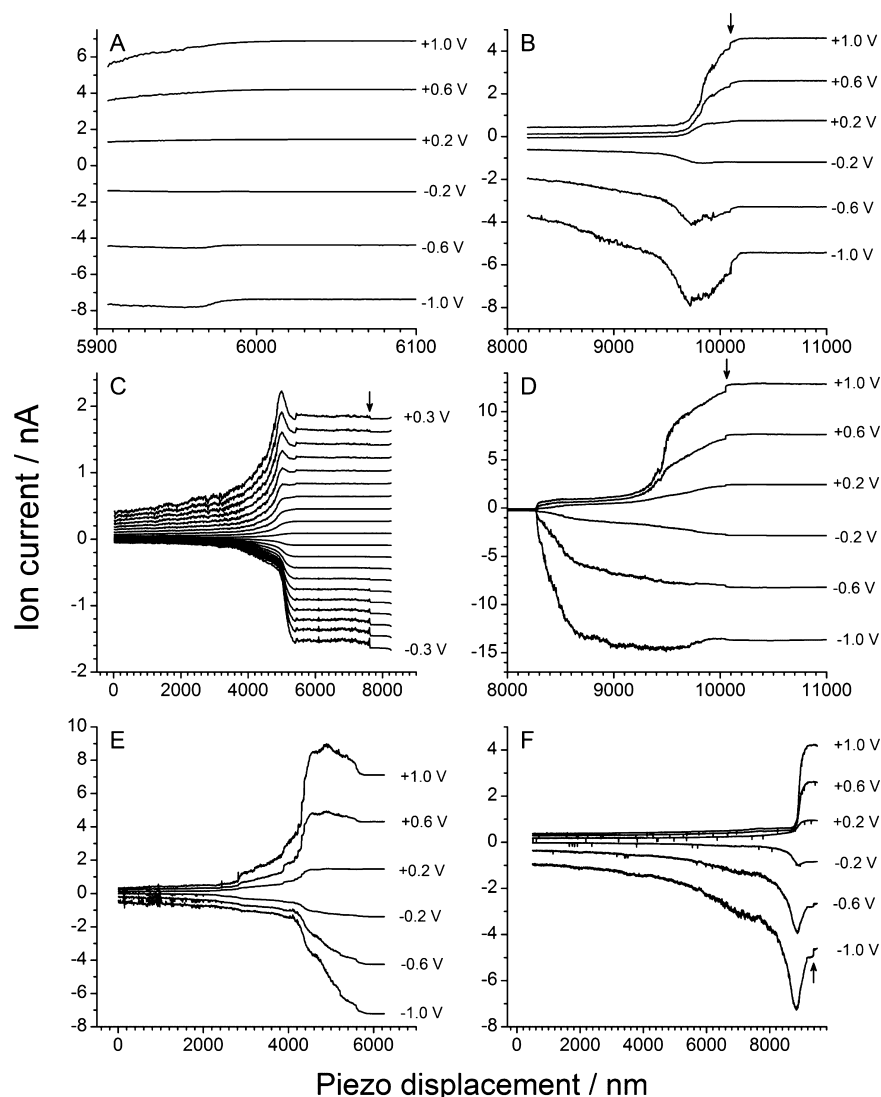


Figure 3. Ion current over glass and decane. (A) 150 mM NaCl, glass. It is not possible to approach glass closely because the nanopipette crashes into it and breaks, but the ion current for negative capillary voltage still exhibits an increase. (B) 150 mM NaCl, decane. The tip repels decane and has to move micrometers in order to reduce the gap through which the ion current flows. (C) 150 mM NaCl, decane, 10 ppm w/v polylysine. The polarity of the ion current increase is reversed. (D) 150 mM NaCl, 1 mM HCl, decane. Effect persists with neutral glass surface charge. (E) 100 mM CaCl₂, decane. CaCl₂ reverses the polarity. (F) 150 mM LiCl, decane. LiCl enhances the effect. Examples of jump-in events of the decane to the pipet are arrowed.

3. RESULTS

3.1. Intrinsic Forces. Nanopipettes can approach solid condensed polystyrene surfaces quite safely until the ion current decreases to a large percentage of its value in bulk as shown in Figure 2. Approaches to glass tend to crash the nanopipettes at only a 5% decrease in positive ion current though, indicating that glass surfaces are strongly attracted to the nanopipette tip at a length scale of the aperture radius, i.e., from tens of nanometers. In contrast the nanopipette tip can get very close indeed to the surface of a decane droplet immersed in saline without crossing the interlayer. Beyond 99%, decreases in ion current are possible because of the strong intrinsic repulsion between the pipet and the decane and because the surface of the decane droplet is completely free to move. As seen in Figure 3, decane surfaces move many micrometers during the course of such approaches. The lack of an initial large drop in current over the distance of an aperture radius indicates the surface is pushed away from a distance of at

least 20 nm by the nanopipette, with this gap only slowly decreasing during the approach. Unlike approaches to solid materials, like glass and polystyrene which are not free to move, approaches to decane also exhibit jump-up events soon after the pipet first encounters the vicinity of the surface. These are the small yet sudden changes in ion current near the beginnings of many of the approach curves to decane, marked by arrows in Figure 3. These sharp changes represent an initial attraction of the decane–saline interlayer to the nanopipette tip, indicating that the intrinsic force between decane and glass in saline is initially attractive and becomes repulsive only when the gap is less than an equilibrium separation.

We saw similar results for live cells as for decane, with nanopipettes maintaining a gap while pushing cell membranes micrometers or tens of micrometers. At very close separations ion current increases were sometimes seen with negative capillary voltages as shown in Figure 4, but generally the ion current decreases in magnitude when approaching cells for

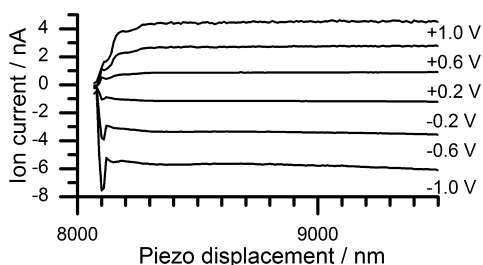


Figure 4. Ion current over COS7 cell in L-15 medium. The cell is pushed micrometers before the gap becomes small enough for the same ion current phenomenon to occur.

either polarity. Extended approaches to cells imply that a nanopipette applies a force at a distance that pushes the cell while maintaining a gap through which an ion current can flow, as in decane. This means that a continuously variable range of relatively weak forces can be applied to the cell by varying the set point of ion current decrease at which the nanopipette stops its approach. At set points of $<0.7\%$ cells do not appear to be perturbed at all by the pipet. The weak forces at slightly higher set points can therefore be used to visualize the cytoskeleton, for example, by pushing the membrane against it as shown in Figure 5, without damaging the live cell.

3.2. Ion Current Enhancement. We first noticed a seemingly anomalous increase in nanopipette ion current next to polystyrene in 150 mM NaCl, which is approximately physiological ionic strength and hence a standard SICM pipet solution. Under these conditions the current increases when the capillary electrode is negative, beginning at about a tip radius away from the surface. Suspecting the effect was related to electroosmotic flow, we added polylysine to the solution to reverse the polarity of the surface charge of the glass pipet. Adding polylysine reverses the polarity of the effect, as would be expected if electroosmotic flow was involved. The effect increases with decreasing ionic strength: No ion current increases are seen at 1500 mM but are large at 15 mM. Typical results from our experiments illustrating these effects are shown in Figure 2.

When approaching glass the ion current for a negative pipet electrode also increased, as in Figure 3A, but these experiments were hampered by the instability mentioned in the previous section. In order to more reliably investigate the ion current effect and the extent of the forces involved, we repeated these series of experiments with the approach of droplets of decane submerged in 150 mM NaCl. The other panels in Figure 3 show typical results for nanopipette approaches to decane: The changes in ion current are very similar to the polystyrene approaches, but rather than the approach taking tens of nanometers, over decane it usually takes micrometers or tens of micrometers because the decane surface moves away from the tip as the gap between it and the nanopipette decreases. This nanopipette/saline/decane geometry has the major benefit of not crashing the pipettes, and so we used it to conduct further tests. The effect of adding polylysine was the same as over polystyrene. To see if the effect requires electroosmosis driven by surface charge, we lowered the pH to below the pK_a (3.5) of the glass, and it was found that it does not; the ion current increase persists at $pH = 3$. We also tested different ions: A reversal of the ion current effect is seen with $CaCl_2$ and an enhancement with $LiCl$ (Figure 3). We include typical voltage–current cross sections in the Supporting Information.

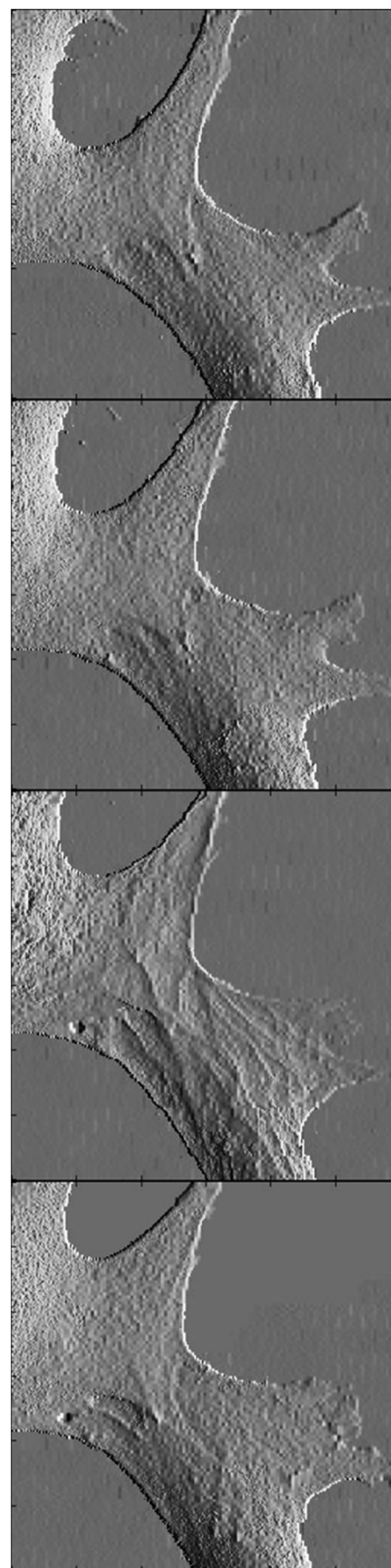


Figure 5. SICM scans of a P4 neuron at ion current decreases of 0.6% (first, second, and fourth scans) and 3.0% (third scan), for which the tip–cell gap is 20–25 nm. An impression of the cytoskeleton holding the membrane up against the nanopipette can be seen in the third scan as it pushes the cell down 16% from 5.5 to 4.6 μm . After this, the cell recovers unperturbed. These 30 μm scans are plotted as $\arctan(d/dx(z(x,y)/\mu m)*25)$, which shows a shadow-like relief easy to interpret visually.

4. DISCUSSION OF INTRINSIC FORCES

Compared to the more accurately calibrated atomic force microscope (AFM)⁷ or surface force apparatus (SFA),⁸ the nanopipette method provides some crucial additional information about the absolute size of the gap between surfaces, in the magnitude of the remaining ion current. This confirms that glass repels the saline–decane interlayer, in agreement with previous work using silica spheres mounted on AFM cantilevers.⁷ Nevertheless, the pattern of interaction across saline in our results is not simple: Glass attracts glass and is initially weakly attracted to decane. But the glass tip repels the saline–decane interlayer as the gap narrows, and the same applies to cells (c.f. Figures 4 and 5). Furthermore, we find these interactions are completely independent of voltage and so must be due to intrinsic colloidal forces rather than electrostriction, which can electroporate cell membranes.⁹

4.1. Patch-Clamping, Pipet–Cell Interaction, and Cell Adhesion Are All Governed by the Same Force Field.

The intrinsic interactions of nanopipettes are critically relevant to their use when mapping surfaces by SICM. It is desirable to detect the surface from as far away as possible, and in practice this means from when the decrease in ion current is just discernible above background noise (for a nanopipette filled with 150 mM NaCl, a typical ion current is 500 ± 1.15 pA noise below 5 kHz for a 100 mV offset), at which time the gap is approximately one aperture radius and tens of nanometers. Our results indicate that at these distances, decane and probably the cell membrane are slightly attracted to the glass tip. Then as the gap closes to less than tens of nanometers and down to nanometer separations, the tip intrinsically repels both decane and membrane. It is this repulsion that allows noncontact mapping of cells by SICM, even when pushing sufficiently to displace the cell membrane slightly.

This same regime of repulsion causes the force barrier to gigaseal formation. A detailed consideration of patch-clamping procedures, in Supporting Information, therefore allows us estimate that the joining pressure of borosilicate glass to cell membrane is ~ 8 kPa. Multiplying this pressure by the surface area of the face of the tip, outside and inner diameters of 100 and 50 nm, respectively, indicates the maximum intrinsic repulsion between the glass and the membrane is 47 pN.

4.2. Complicated Force Field Can Be Rationalized by Accounting for the High Permittivity of the Double Layer of the Glass at the Nanopipette Tip. In this section we present a possible origin for the repulsion of cell membranes in saline from glass, the force that allows noninvasive SICM and that needs to be overcome for gigaseals to be formed. The discussion also predicts that during the approach to the cell, the membrane will first be very slightly attracted to the nanopipette tip.

Some predictions for the force between a glass nanopipette and a glass slide immersed in saline can be drawn from existing experimental evidence in colloid science. There is no component to the force from electrostatic repulsion of the double layers at the surfaces until they approach to within a Debye length, which at 150 mM salt concentration is 0.78 nm. Because the repulsion of the double layers at the glass surfaces is screened in this way, the sign of the overall force at larger separations is determined by the component of the force due to the van der Waals interaction, which for glass/saline/glass is entirely attractive because the permittivity of the intervening saline is not intermediate to the permittivities of the glass at

either side.¹⁰ However the same is true for decane/saline/glass, implying that in the (standard) Derjaguin–Landau–Verwey–Overbeek (DLVO) theory,¹¹ a monotonic attraction would be expected^{12,13} when we in fact observe that glass repels decane across saline. Therefore the assumptions made in the DLVO theory must be reassessed slightly: We assert that interlayers, for example, the electrical double layer, do not only contribute to electrostatic forces at separations of the size of the Debye length but also affect the sign and magnitude of the Hamaker constant across gaps of tens of nanometers because of the drastic variations in permittivity across these interlayers. At even wider separations the effect would be averaged out by phase differences due to retardation.

When saline is the medium the double layers adjacent to charged surfaces are important because they have very high capacitance and hence permittivity. The differential capacitance of 100 mM sodium chloride is about $0.28 \text{ F}\cdot\text{m}^{-2}$.¹⁴ With a Debye length of about a nanometer, this corresponds to a relative permittivity of 3200. Thus at close separations, the substance of the nanopipette itself is probably completely irrelevant to the Hamaker constant of the van der Waals interaction, H , compared to the double layer it induces. Assuming non-retardation and direct additivity, we can make the Derjaguin approximation of integrating over height the energy per unit area times the differential cross-sectional area,¹⁵ and this affirms that the tip dominates the interaction, not just because it is closest but also because of the sharp differential change in cross-sectional area there. Given that the force per unit area between two flat surfaces separated by a distance S is $H/6\pi S^3$ ¹⁰ and at the tip the cross-sectional area of the double layer abruptly changes, over the small distance of the Debye length, d , from zero to A , the area of the face of the tip of the nanopipette, the total van der Waals force between the tip and a surface will simply be $HA/6\pi S^3$, where H is the Hamaker constant for the surface/saline/double-layer system. Note that it is the assertion here of the importance of the double layer to the sign and magnitude of the van der Waals force rather than only to electrostatic double-layer repulsion that is unusual and interesting. The type of derivation required for interactions including surface layers is given by Israelachvili.¹⁶

Inverting the formula above allows us to estimate the Hamaker constant for the cell-membrane/saline/double-layer system: A pressure of 8 kPa at a separation of 3 nm gives a Hamaker constant of -4 zJ . The magnitudes of the corresponding constants for many other combinations of materials are comparable,¹⁷ so this value is not unreasonable. Assuming the same Hamaker constant for decane/saline/double-layer and a surface tension of $50 \text{ mN}\cdot\text{m}^{-1}$,¹⁸ this pressure translates to a radius of curvature of $12.5 \mu\text{m}$. This agrees with the fact that the decane does not envelope the nanopipette. It is important to remember though that for decane and cell membranes, the Hamaker constant is actually a function of distance. The jump-in events in Figure 3 suggest that at larger separations it even has opposite sign, corresponding to slight attraction.

For systems consisting of two infinite half-spaces separated by a third substance, the van der Waals force pulls the half-spaces together unless the refractive index and permittivity of the intervening medium are intermediate to those on either side. Thus for the double-layer/saline/double-layer system (for the reasons above this description substitutes ‘double-layer’ for ‘glass’), the force is expected to be attractive. The Hamaker constant for this interaction will probably be higher than that

for silica interacting across pure water, +5 zJ,¹⁷ because of the higher conductivity of the saline solution. Because of the symmetry of this system, the sign of the force in this case does not depend upon whether it is the relative permittivity of the glass or the double layer that dominates. Thus quite strong monotonic attraction is expected between a glass nanopipette and a glass coverslip, which explains why this configuration is unstable. For decane and polystyrene the distinction between the glass of the nanopipette and its associated double layer matters, because the system is no longer symmetric in this aspect. The (relative) permittivities of decane and polystyrene are about 2.0 and 2.5, respectively,¹⁹ less than the permittivity of the saline, ~78,²⁰ which is in turn less than the permittivity of the double layer next to the glass, ~3200. So the Hamaker constants of these substances adjacent to/saline/double-layer(glass) are expected to be repulsive in this analysis. (Using the permittivity of the glass, only around 3.8,¹⁹ would have suggested the force was attractive.) Therefore, taking account of the double layer can reconcile the repulsion between decane and the nanopipette tip observed experimentally with the theory of the van der Waals interaction. At larger separations the Hamaker constant must be a stronger function of the permittivities of the bulk substances rather than the interlayers between them.

Most phospholipids have head groups with both positive and negative charges, so for cell membranes, as for decane, an attractive van der Waals interaction to glass would be expected initially because the saline would have higher permittivity than both the hydrophobic portion of the bilayer and the glass. However, when the interfaces approach more closely, the permittivity of the double layer of the glass would override that of its substrate, giving a repulsive force as for decane.

If the colloidal interaction prior to adsorption of membrane to glass is repulsive, cells in suspension would need a strategy to adhere to it. According to the scheme outlined above, the cell could utilize the weak attractive force at slightly larger separations, spreading out to maximize the available force from this weaker pressure. It would then send down perhaps just one or two narrow podia to push through the stronger repulsive pressure at closer separations and thereby anchor to the surface.

Equally important are the technological implications of double-layer induced repulsion of an apolar surface: This repulsion could be useful for nanoscale machines²¹ and macroscopic devices requiring an economical implementation of low friction in liquid at low applied pressures.

4.3. Steric Contribution of the Interlayer between Saline and Flat Surfaces. To varying extents, the cell membrane shares another relevant feature of the oil-saline interlayer: The results of Ikeda et al.¹⁸ and Motomura et al.²² indicate that adjacent to the decane is a layer of pure water about 14 molecules thick. This thickness does not correspond to the quoted subangstrom distance between the dividing planes for excess moles of decane and water but instead to the height of solution from which salt would have to be evacuated to satisfy the calculated interfacial density of $-0.6 \mu\text{mol}\cdot\text{m}^{-2}$ at 150 mM,¹⁸ a distance of ~4 nm. The average distance between chloride ions in bulk 150 mM NaCl is around 2 nm, i.e., around seven water molecules, so the magnitude of this result is not implausible. The assumption of water purity in this interlayer follows from the almost complete independence of the energy of interface formation with molality, a large value of $80 \text{ mJ}\cdot\text{m}^{-2}$.¹⁸ Assuming that locally flat geometry and low variation

in surface charge density are the determining factors in the formation of this interlayer,^{23–25} then these same interlayers of water molecules would explain the dependence of apparent contact position between hard, flat surfaces on the intermediate salt concentration. For example, sapphire,²⁶ mica,²⁷ and alumina²⁸ surfaces exhibit strong repulsion significantly offset from hard contact, and adding water generates plasticity in clays^{29,30} and can force expansions in certain layered minerals.^{27,31}

In terms of absence of ions the interlayer is much thicker than the gap between the null-excess dividing planes. This means the water interlayer must be slightly expanded relative to the rest of the solution. The consequent hydrogen-bond lability would enhance proton transfer. Moreover, at the exterior edge of this interlayer an excess concentration of chloride ions is likely,³² because of their greater susceptibility to hydrogen bonding than other ions.³³ It is known that the pH, at which a surface has no net charge from specifically adsorbed charges, is not the same as the isoelectric point (the pH at which the shear plane has no net charge),³⁴ and a layer of chloride ions would cause this. This chloride and the enhanced proton transfer would give the interlayer high lateral conductivity, of relevance to the next section. Sequestration of chloride ions is consistent with the idea of a negative potential developing on apolar surfaces, previously hypothesized¹² to account for the repulsion of apolar surfaces from glass.^{12,13} Cholesterol seems to enhance this type of interlayer,³⁵ which would allow cells to modulate their colloidal interactions to some extent.

5. ION CURRENT ENHANCEMENTS CAN BE EXPLAINED BY THE EMERGENCE OF ELECTROOSMOTIC FLOW SEPARATION

The occlusion of the tip aperture by a surface shuts off the ion current as the gap closes, as would be expected for uniformly conductive solution. As we have shown however, the ion current can actually increase when a nanopipette approaches some surfaces under certain conditions. This happens when a nanopipette with a negative voltage bias approaches a polystyrene surface or a decane surface. The polarity of the effect is reversed if the negative charges of the silanol groups on the glass surface are reversed by polylysination or if calcium chloride is substituted for sodium chloride. In all cases, the effect increases with the magnitude of the voltage.

It is widespread in the literature to average out interactions with the mean-field approximation. This simplification of the Poisson–Boltzmann equation predicts polarity-dependent changes in concentration at the tip consistent with ion current rectification in a fixed geometry with surface charge.^{36,37} Not using that approximation would be far beyond our computational resources, but we would like to raise objections here that the solution is unlikely to be stable, especially not against electroosmotic flow driven from further up the pipet and that it is inconsistent with an increasing current when the aperture starts to be occluded by a surface. These objections motivate the following suggestion that electroosmotic flow separation, the emergent structure of diffusely concentric flows of anions and cations, would be a stable steady-state better able to explain our results.

A relevant consideration is the velocity of electroosmotic flow. Often in microfluidic devices, electroosmosis is used to drive flow. This requires low salt concentrations of <1 mM, as it is usually not possible in those configurations to apply a large enough voltage to generate electroosmotic flow at higher salt

concentrations, due to water electrolysis at metal electrodes. However, in a nanopipette the electric field at the tip aperture can be very high indeed for moderate applied voltages due to the much smaller scale of the insulating geometry. Thus, even at a high salt concentration, like 250 mM NaCl, the high field generates an electroosmotic flow speed of at least $1.6 \text{ mm}\cdot\text{s}^{-1}\cdot\text{V}^{-1}$ at the tip aperture (calculated from data in Rodolfa et al.).³⁸ This is quite fast, especially in the context that electroosmosis is usually completely negligible at concentrations $>10 \text{ mM}$.³⁹ The theoretical electroosmotic flow speed is also high; using the very consistent data in Jednačák et al.⁴⁰ and Pelton et al.⁴¹ and the surface charge formula with the suggested approximation⁴⁰ of constant charge produced by boronol groups, we derive a ζ potential for borosilicate glass in 150 mM NaCl of -22.9 mV , which would give an electroosmotic flow per volt of $15.8 \text{ mm}\cdot\text{s}^{-1}\cdot\text{V}^{-1}$ for a field of $10^6 \text{ V}\cdot\text{m}^{-1}$ per volt at the tip. Now, the phenomenon of electroosmosis is generated by viscous friction of solvated ions against water molecules, which implies that ions flowing against electroosmosis will also experience viscous friction of the same order of magnitude. We can calculate the speeds of the sodium and chloride ions at the tip aperture using their respective limiting conductivities³³ of 50.10 and $76.35 \text{ S}\cdot\text{cm}^2\cdot\text{mol}^{-1}$. A current of 5 nA at 1 V through an aperture of 50 nm diameter in 150 mM NaCl is equivalent to the sodium ions moving at $70 \text{ mm}\cdot\text{s}^{-1}\cdot\text{V}^{-1}$ and the chloride ions moving at $106 \text{ mm}\cdot\text{s}^{-1}\cdot\text{V}^{-1}$ the other way. Thus the velocity of the net electroosmotic flow calculated above is a sizable fraction of the flow speeds of the ions.⁴² These considerations suggest that in some situations, a diffuse structure to the flow field of anions and cations emerges; concentric electroosmotic flows in opposite directions through the nanopipette aperture. This would reduce the average viscous friction on ions, allowing a higher overall ion current. If the electroosmotic flow did separate, then the local ratios of this flow field with those of the ions would be even higher than the net fraction calculated above using the approximation of uniformity. This cooperativity would stabilize the effect, and also its emergence would be promoted by a double layer in cylindrical symmetry. We estimate the energy scales involved in the Supporting Information.

The asymmetry of nanopipette currents with voltage and their enhancements at surfaces can both be explained by this low-energy phenomenon: For sodium chloride, when the sodium counterions at the inside surface of the tip aperture flow outward, the electroosmotic flow that is pulled along with them hinders the entry of chloride co-ions into the tip aperture. Outside of the tip there is a bottleneck for the inward flow of co-ions because the electric field is not as strong there as just inside the narrow constriction of the tip, where the electroosmotic flow is driven. So electroosmotic flow separation would be suppressed, and the overall ion current reduced. In the opposite polarity however, when the counterions flow inward, the situation is not the same. Although the flow of co-ions is still opposed by hydrodynamic friction from the movement of the counterions, the electric field inside the tip is high enough to overcome this. The result is that in this polarity the electroosmotic flow would sometimes stably separate into diffusely concentric flows of anions and cations, enhancing the overall ion current. The hypothesis is simply that this process is enhanced when the ions driving the dominant electroosmosis (the sodium counterions in the case of sodium chloride) flow inward and largely disrupted when they flow outward. This separated flow profile would be promoted by a flat surface at a

certain distance from the nanopipette tip, explaining the ion current enhancement we see when the flow of ions driving the main electroosmosis is inward. Further enhancement would be seen for surfaces with high lateral conductivity. The ion current enhancement remains when the silanol groups are (dynamically) reprotonated (Figure 3D). This strongly supports the idea of emergent flow structure over changes in tip ion concentration.^{36,37}

The adsorption of Ca^{2+} to silica⁴³ reverses the surface charge. Polylysine does the same and also increases its magnitude. Thus in these solutions the primary electroosmotic flow is driven more by the chloride co-ions, reversing the polarity of the ion current enhancement as we and others⁴⁴ observe. Conversely, lithium counterions seem to be more effective than sodium ions at generating a primary electroosmotic flow, as for 15 vs 150 mM NaCl. At 1.5 M the current may be limited by heating, or the polystyrene–saline interlayer may be destroyed.

In summary we have argued that the high-salt, high-electric field regime of these experiments means that ion–ion interactions cannot be averaged out by a mean-field approximation³⁹ and that this generates a new electrokinetic effect, which we term electroosmotic flow separation. For slow approaches around 1 nm/s , the ion current is a fairly reproducible function of distance. However, when used to map surfaces, nanopipettes are typically moved downward at least a 1000 times faster. At these speeds the ion current as a function of gap distance is by no means the same for every approach, even to the extent that sometimes the current increases do not occur or only occur as the pipet moves away. Thus the onset of the underlying process indicated by ion current enhancement (i.e., the hypothesized electroosmotic flow separation) must be sensitive to nanoscopic conditions and mesoscopic fluctuations. As the power throughput is also known, this could make a good test system for studying nonequilibrium structural emergence.

6. CONCLUSIONS

Interactions between surfaces in strong ($>1 \text{ mM}$) electrolyte solutions are critical to life and biology at all levels, from organs to organelles, but do not obviously conform^{12,13,45} to the DLVO theory¹¹ successful at lower salt concentrations. We have investigated two reasons: the decane–saline interlayer and the double-layer contribution to the van der Waals force. Our results lead us to conclude that the permittivity of interlayers, and of double layers in particular, can be determining factors for the Hamaker parameter at separations of the order of 10 nm in strong solutions of electrolytes. This can explain the longer range (tens of nanometers in the context of a 0.78 nm Debye length) repulsions and attractions that we and others^{7,45} observe between glass and interfaces across saline. This encompasses many phenomena including patch clamping and biological modulation of coagulation.

We have also highlighted a new physical phenomenon in the same geometry that is relevant to any study of ionic conduction through constrictions—electroosmotic flow separation. When a nanopipette approaches an insulating surface, the occlusion of the aperture usually decreases the ion current. Under certain conditions though, it increases instead. Extensive investigation has led us to hypothesize this is due to structural emergence of diffuse separation in the flow fields of anions and cations, enhanced by lateral conductivity of the interlayer adjacent to the insulator.

■ ASSOCIATED CONTENT

■ Supporting Information

Voltammograms and discussions of gigaseal formation and energy scales. This material is available free of charge via the Internet at <http://pubs.acs.org>.

■ AUTHOR INFORMATION

Corresponding Author

rwc25@cam.ac.uk; dk10012@cam.ac.uk

Notes

The authors declare no competing financial interest.

■ ACKNOWLEDGMENTS

This work was also funded by a U.K. Research Council. We thank Dr. S. Antolin, Professor J. P. Hansen, and Dr. P. Jönsson for critical comments. R.W.C. thanks Christ's College Cambridge for a Research Fellowship. O.R. thanks the RSC Analytical Chemistry Trust Fund.

■ REFERENCES

- (1) Hansma, P. K.; Drake, B.; Marti, O.; Gould, S. A.; Prater, C. B. *Science* **1989**, *243*, 641.
- (2) Shevchuk, A. I.; Frolenkov, G. I.; Sánchez, D.; James, P. S.; Freedman, N.; Lab, M. J.; Jones, R.; Klenerman, D.; Korchev, Y. E. *Angew. Chem.* **2006**, *118*, 2270.
- (3) Mann, S. A.; Hoffmann, G.; Hengstenberg, A.; Schuhmann, W.; Dietzel, I. D. *J. Neurosci. Methods* **2002**, *116*, 113.
- (4) Novak, P.; Li, C.; Shevchuk, A. I.; Stepanyan, R.; Caldwell, M.; Hughes, S.; Smart, T. G.; Gorelik, J.; Ostanin, V. P.; Lab, M. J.; Moss, G. W. J.; Frolenkov, G. I.; Klenerman, D.; Korchev, Y. E. *Nat. Methods* **2009**, *6*, 279.
- (5) Gorelik, J.; Zhang, Y.; Shevchuk, A. I.; Frolenkov, G. I.; Sánchez, D.; Lab, M. J.; Vodyanoy, I.; Edwards, C. R. W.; Klenerman, D.; Korchev, Y. E. *Mol. Cell. Endocrinol.* **2004**, *217*, 101.
- (6) Ying, L.; Bruckbauer, A.; Rothery, A. M.; Korchev, Y. E.; Klenerman, D. *Anal. Chem.* **2002**, *74*, 1380.
- (7) Mulvaney, P.; Perera, J. M.; Biggs, S.; Grieser, F.; Stevens, G. W. *J. Colloid Interface Sci.* **1996**, *183*, 614.
- (8) Israelachvili, J. N.; Adams, G. E. *Nature* **1976**, *262*, 774.
- (9) Bae, C.; Butler, P. J. *Biomech. Model. Mechanobiol.* **2008**, *7*, 379.
- (10) Hunter, R. J. *Introduction to Modern Colloid Science*; Oxford University Press: Oxford, 1996.
- (11) Verwey, E. G. W.; Overbeek, J. T. G. *The Theory of the Stability of Lyophobic Colloids*; Elsevier: Amsterdam, 1948.
- (12) Hartley, P. G.; Grieser, F.; Mulvaney, P.; Stevens, G. W. *Langmuir* **1999**, *15*, 7282.
- (13) Clasohm, L. Y.; Vakarelski, I. U.; Dagastine, R. R.; Chan, D. Y. C.; Stevens, G. W.; Grieser, F. *Langmuir* **2007**, *23*, 9335.
- (14) Grahame, D. C. *Chem. Rev.* **1947**, *41*, 441.
- (15) Derjaguin, B. *Kolloid Zeitschrift* **1934**, *69*, 155.
- (16) Israelachvili, J. N. *Proc. R. Soc. Lond. A* **1972**, *331*, 39.
- (17) Bergström, L. *Adv. Colloid Interface Sci.* **1997**, *70*, 125.
- (18) Ikeda, N.; Aratono, M.; Motomura, K. *J. Colloid Interface Sci.* **1992**, *149*, 208.
- (19) *Dielectric Constants of Various Materials*; Delta Controls: Shreveport, LA; <http://www.deltacnt.com/99-00032.htm> (accessed December 12, 2012).
- (20) Stogryn, A. *IEEE Trans. Microwave Theory Tech.* **1971**, *19*, 733.
- (21) Feynman, R. J. *Microelectromech. Syst.* **1993**, *2*, 4.
- (22) Motomura, K.; Iyota, H.; Aratono, M.; Yamanaka, M.; Matuura, R. *J. Colloid Interface Sci.* **1983**, *93*, 264.
- (23) Teschke, O.; Filho, J. F. V.; de Souza, E. F. *Chem. Phys. Lett.* **2010**, *485*, 133.
- (24) Miranda, P. B.; Xu, L.; Shen, Y. R.; Salmeron, M. *Phys. Rev. Lett.* **1998**, *81*, 5876.

- (25) Xu, D.; Liechti, K. M.; Ravi-Chandar, K. *Langmuir* **2009**, *25*, 12870.
- (26) Horn, R. G.; Clarke, D. R.; Clarkson, M. T. *J. Mater. Res.* **1988**, *3*, 413.
- (27) Pashley, R. M. *J. Colloid Interface Sci.* **1981**, *83*, 531.
- (28) Ducker, W. A.; Xu, Z.; Clarke, D. R.; Israelachvili, J. N. *J. Am. Ceram. Soc.* **1994**, *77*, 437.
- (29) Velamakanni, B. V.; Chang, J. C.; Lange, F. F.; Pearson, D. S. *Langmuir* **1990**, *6*, 1323.
- (30) Lewis, J. A. *J. Am. Ceram. Soc.* **2000**, *83*, 2341.
- (31) Norrish, K. *Faraday Discuss.* **1954**, 120–134.
- (32) Tian, C. S.; Shen, Y. R. *Proc. Natl. Acad. Sci. U.S.A.* **2009**, *106*, 15148.
- (33) Atkins, P. W. *Physical Chemistry*; Oxford University Press: Oxford, 1994.
- (34) Adamson, A. W.; Gast, A. P. *Physical Chemistry of Surfaces*; John Wiley and Sons: New York, 1997.
- (35) Lis, L. J.; McAlister, M.; Fuller, N.; Rand, R. P.; Parsegian, V. A. *Biophys. J.* **1982**, *37*, 657.
- (36) Wei, C.; Bard, A. J.; Feldberg, S. W. *Anal. Chem.* **1997**, *69*, 4627.
- (37) White, H. S.; Bund, A. *Langmuir* **2008**, *24*, 2212.
- (38) Rodolfa, K. T.; Bruckbauer, A.; Zhou, D.; Shevchuk, A. I.; Korchev, Y. E.; Klenerman, D. *Nano Lett.* **2006**, *6*, 252.
- (39) Bazant, M. Z.; Kilic, M. S.; Storey, B. D.; Ajdari, A. *Adv. Colloid Interface Sci.* **2009**, *152*, 48.
- (40) Jednačák, J.; Pravdič, V.; Haller, W. J. *Colloid Interface Sci.* **1974**, *49*, 16.
- (41) Pelton, R. H.; Allen, L. H. *J. Colloid Interface Sci.* **1984**, *99*, 387.
- (42) Ai, Y.; Zhang, M.; Joo, S. W.; Cheney, M. A.; Qian, S. J. *Phys. Chem. C* **2010**, *114*, 3883.
- (43) Iler, R. K. *J. Colloid Interface Sci.* **1975**, *53*, 476.
- (44) He, Y.; Gillespie, D.; Boda, D.; Vlassiok, I.; Eisenberg, R. S.; Siwy, Z. S. *J. Am. Chem. Soc.* **2009**, *131*, 5194.
- (45) Dagastine, R. R.; Chau, T. T.; Chan, D. Y. C.; Stevens, G. W.; Grieser, F. *Faraday Discuss.* **2005**, *129*, 111.